J Neurophysiol 110: 19–32, 2013.
First published April 10, 2013; doi:10.1152/jn.00686.2012.

Comparison of abstract decision encoding in the monkey prefrontal cortex, the presupplementary, and cingulate motor areas

Katharina Merten and Andreas Nieder
Animal Physiology, Institute of Neurobiology, University of Tübingen, Germany

Submitted 7 August 2012; accepted in final form 4 April 2013

Merten K, Nieder A. Comparison of abstract decision encoding in the monkey prefrontal cortex, the presupplementary, and cingulate motor areas. *J Neurophysiol* 110: 19–32, 2013. First published April 10, 2013; doi:10.1152/jn.00686.2012.—Deciding between alternatives is a critical element of flexible behavior. Perceptual decisions have been studied extensively in an action-based framework. Recently, we have shown that abstract perceptual decisions are encoded in prefrontal cortex (PFC) neurons (Merten and Nieder 2012). However, the role of other frontal cortex areas remained elusive. Here, we trained monkeys to perform a rule-based visual detection task that disentangled abstract perceptual decisions from motor preparation. We recorded the single-neuron activity in the presupplementary (preSMA) and the rostral part of the cingulate motor area (CMAr) and compared it to the results previously found in the PFC. Neurons in both areas traditionally identified with motor planning process the abstract decision independently of any motor preparatory activity by similar mechanisms as the PFC. A larger proportion of decision neurons and a higher strength of decision encoding was found in the preSMA than in the PFC. Neurons in both areas reliably predicted the monkeys' decisions. The fraction of CMAr decision neurons and their strength of the decision encoding were comparable to the PFC. Our findings highlight the role of both preSMA and CMAr in abstract cognitive processing and emphasize that both frontal areas encode decisions prior to the preparation of a motor output.

monkey; single-unit recording; decision making; frontal cortex; detection task

DECISIONS ARE CHOICES BETWEEN alternatives, often in a situation of uncertainty. Perceptual decisions require an evaluation of ambiguous or noisy sensory information and a transformation into categorical judgments to influence behavior. Such judgments cannot be explained alone by properties of early sensory area neurons that primarily reflect the physical properties of the stimulus (de Lafuente and Romo 2005; Mountcastle et al. 1969). Subjective judgments require integration of the sensory information with internal goals, experiences, and expectations. Flexible decisions are thus regarded as a hallmark of higher cognition.

The neuronal implementation of perceptual decisions has been addressed at various cortical and subcortical structures. Decision correlates were found in many areas, such as the prefrontal cortex (PFC) (Hernández et al. 2010; Kim and Shadlen 1999; Lemus et al. 2009; Romo et al. 2004), the frontal eye field (Gold and Shadlen 2003), the medial and ventral premotor cortexes (de Lafuente and Romo 2005, 2006; Hernández et al. 2002), the lateral intraparietal area (LIP) (Roitman and Shadlen 2002; Shadlen and Newsome 2001), and the superior colliculus (Gold and Shadlen 2000; Horwitz and Newsome 1999). These studies regarded perceptual decisions as an intention to pursue a particular action associated with a percept (intentional framework) (Gold and Shadlen 2007; Shadlen et al. 2008).

However, a different neuronal network might emerge if perceptual decisions are dissociated from action preparation. Traditionally, the PFC at the apex of the cortical hierarchy is thought to be involved in the processing of abstract cognitive variables (Freedman et al. 2001; Miller and Cohen 2001; Nieder 2012; Wallis et al. 2001). We recently investigated the representation of abstract perceptual decisions in the PFC of rhesus monkeys (Merten and Nieder 2012) in a rule-based visual detection task that allowed a clear dissociation of a decision about the presence or absence of a stimulus from motor preparation. The neuronal representation evoked by abstract decisions was different from the processing mechanisms previously found for action-based detection decisions (de Lafuente and Romo 2005). In addition to the neurons actively modulating their discharges for "yes" decisions (stimulus present), we found a second set of neurons actively modulating their responses for "no" decisions (stimulus absent). The emergence of "no" neurons seems to be characteristic for highly abstract processing, because these responses are not based on sensory input and are not triggered by motor preparations.

The present work explores and compares the encoding of abstract detection decisions in areas of the frontal cortex traditionally identified with motor planning. Of particular interest is the presupplementary motor area (preSMA), because this area appears to be responsible for more abstract, cognitive, high-level motor functions (Picard and Strick 1996; Shima et al. 1996; Tanji 1994). Moreover, the rostral part of the cingulate motor area (CMAr) is a candidate to be involved in cognitive processing, because just as the preSMA, CMAr receives direct input from the PFC (Bates and Goldman-Rakic 1993; Lu et al. 1994; Wang et al. 2005). Moreover, a recent study describes the involvement of this area in abstract rule processing (Vallentin et al. 2012). We show that neurons in all three areas encode decisions as abstract categories prior to the translation of decisions into motor intentions.

MATERIALS AND METHODS

Behavioral protocol. Two rhesus monkeys (*Macaca mulatta*) were trained on a rule-based visual detection task (Fig. 1*A*). In each randomly selected experimental trial, the monkeys were required to report the presence or the absence of a stimulus dependent on a color cue that instructed a particular motor response. The monkeys initiated a trial by grasping a lever and fixating a central fixation target for 500 ms. A brief stimulus appeared for 100 ms in 50% of the trials. In the other half of the trials, the stimulus was absent. After the delay period (2,700 ms), a color cue was presented. If the monkey correctly

Address for reprint requests and other correspondence: A. Nieder, Animal Physiology, Institute of Neurobiology, Univ. of Tübingen, Auf der Morgenstelle 28, 72076 Tübingen, Germany (e-mail: andreas.nieder@uni-tuebingen.de).

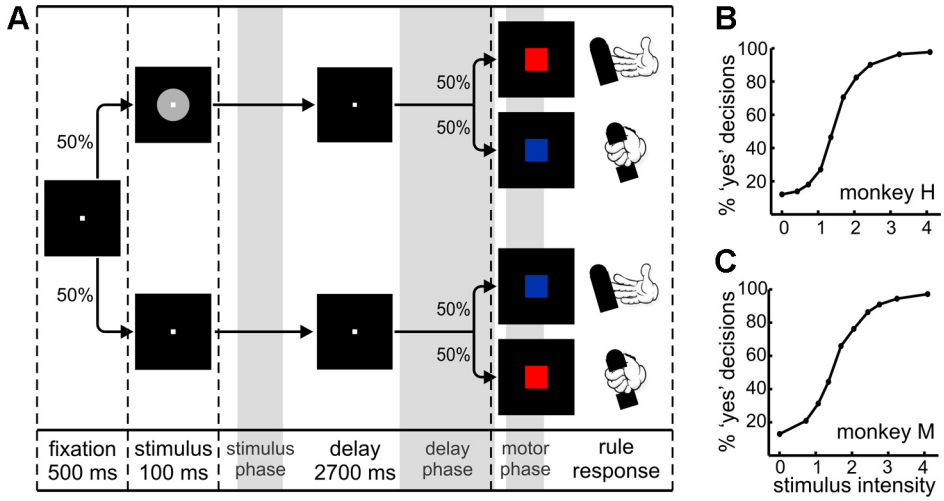

Fig. 1. Rule-based detection task and behavioral performance. *A*: to start a trial, the monkeys grasped a lever and maintained fixation. In 50% of the trials, the monkeys were presented with a gray object, whose intensity varied in nine levels, centered around the perceptual threshold. In the other 50% of the trials, no stimulus was shown. During the delay period, the animals decided about the presence or absence of the stimulus. After the delay, a color cue (50% red, 50% blue) appeared to instruct the appropriate response to a particular decision. After the presentation of a stimulus, a red square cue required the monkeys to release the lever within 1,000 ms to receive a fluid reward, whereas a blue cue demanded the monkey to keep holding the lever for another 1,200 ms. The rule applied in the inverse way in stimulus-absent trials. The protocol ensures that no motor response preparation could take place during the delay period. The gray areas mark the periods of data analysis: stimulus and delay phase during the decision period and the motor phase, after the rule-cue onset. *B* and *C*: psychometric detection curve of the tested stimulus intensities (%visual contrast; visual contrast of 0 indicates absence of the stimulus) for *monkey H* (*B*) and *monkey M* (*C*).

detected the presence of the stimulus, a red square cue required the monkey to release the lever within 1,000 ms to receive a fluid reward. A blue square instructed the monkey to keep holding the lever for 1,200 ms. The rule applied in the inverse way if the absence of the stimulus was detected: blue square–release the bar; red square–keep holding. The monkeys were required to keep their gaze within 1.75° of visual angle of the fixation target during stimulus and delay periods. Eye movements were monitored with an infrared eye-tracking system (ISCAN, Woburn, MA). The CORTEX program (National Institute of Mental Health) was used for experimental control and behavioral data acquisition.

Stimuli. The stimulus consisted of a gray object (4° of visual angle) of three possible shapes: square, circle, hexagon for *monkey H*; cross, triangle, and rhomboid for *monkey M*. The area of the object was kept constant to maintain the visual contrast of the stimulus across different shapes. The stimulus was presented at nine levels of contrast close to the perception threshold (monkey H: 4.1%, 3.2%, 2.4%, 2.0%, 1.7%, 1.4%, 1.1%, 0.7%, 0.4%; *monkey M*: 4.1%, 3.2%, 2.8%, 2.4%, 2.0%, 1.7%, 1.4%, 1.1%, 0.7%), measured with a J16 Digital Photometer (Tektronix, Beaverton, OR).

Neurophysiological recordings. The rhesus monkeys were implanted with a head bolt to maintain the head in a constant position during the sessions to allow for eye movement measurements. All surgeries were performed under sterile conditions while the animals were under general anesthesia. The animals received postoperative antibiotics and analgesics. All procedures were carried out in accordance with the guidelines for animal experimentation approved by the Regierungspräsidium Tübingen, Germany.

We performed extracellular single-cell recordings simultaneously in the lateral PFC, the preSMA, and the rostral part of the CMAr. We used glass-coated tungsten microelectrodes of 1 MΩ impedance (Alpha Omega, Nazareth, Israel). Arrays of four to eight electrodes with 1 mm spacing were inserted during each recording session into the recording chambers. Neurons were selected at random in every recording session; no attempt was made to preselect neurons according to response properties. Signal acquisition, amplification, filtering, and digitalization were accomplished using the Plexon system (Plexon, Dallas, TX). The placement of the recording chambers and the location of the recording sites were reconstructed in stereotactic coordinates using magnetic resonance images of individual monkey brains (Fig. 2). The depth of the recordings was estimated for the different regions: PFC: *monkey H*: 2–4.8 mm, *monkey M*: 2–5.8 mm; preSMA: *monkey H*: 2–5.6 mm, *monkey M*: 2–5 mm; CMAr: *monkey H*: 10–11 mm, *monkey M*: 7–13 mm.

Data analysis. We sorted the spikes offline and studied the responses of all well-isolated neurons. We focused our analysis on two intervals during the decision period: the stimulus phase, a 300-ms period after stimulus onset shifted by the individual response latency of the cell, and the (late) delay phase, a 1,000-ms window starting 1,900 ms after stimulus onset. Moreover, we analyzed the neuronal responses also during the motor phase: a 200-ms interval, which started 100 ms and ended 300 ms after rule-cue onset. Data analysis was performed using MATLAB (MathWorks, Natick, MA). The significance level used in this work is 0.05.

Excluding nonabstract, object feature-selective neurons. A Kruskal-Wallis-test was used to analyze the selectivity of every neuron for the three different types of the presented objects, to ensure that the studied neurons encoded abstract object properties, irrespective of low-level visual features. For this test, hit trials of all intensities were grouped by object type. We found that only few neurons showed significantly ($\alpha = 0.05$) different discharge rates for the object types: (PFC: 5% during the stimulus and delay phase; preSMA: 4% in both intervals of analysis; CMAr: 6% during the stimulus phase and 5% during the delay phase). These cells were excluded from the analysis.

Stepwise linear regression analysis. To investigate the relationship between the firing rates, the monkey's choices, and the stimulus intensities during the decision period, a stepwise linear regression (SLR) analysis was calculated (Draper and Smith 1966; Pardo-Vazquez et al. 2008). We fitted the neuronal activity measured for each single cell during the stimulus and delay phases to a linear function of both the intensity (all tested stimulus intensities) and decision ("yes": hits and false alarms vs. "no": misses and correct rejections). The following equation describes this relationship:

$$FR = a_0 + a_{int} \times INT + a_d \times D$$

The coefficients a_{int} and a_d quantify the dependence of the firing rate (*FR*) on intensity (*INT*) and decision (*D*). Normalized firing rates were used to determine the coefficients (see *Population analysis and normalization*).

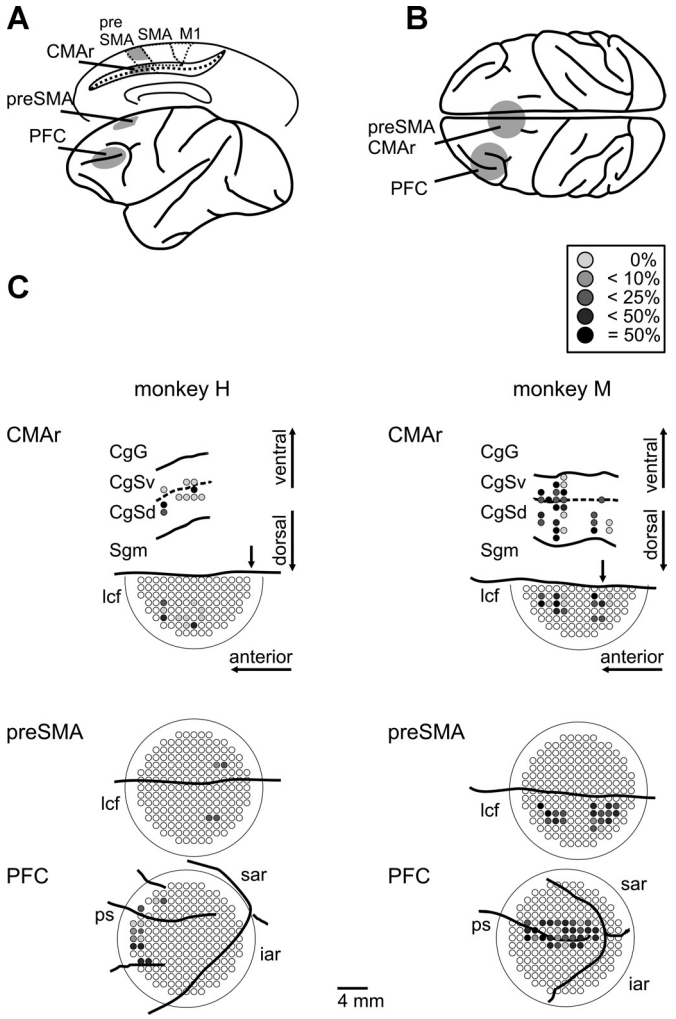

Fig. 2. Recording sites. *A*: medial and lateral view of the monkey brain showing the recording sites in the lateral prefrontal cortex (PFC), presupplementary motor area (preSMA), and the cingulate motor area (CMAr). SMA, supplementary motor area; M1, primary motor cortex. *B*: locations of the two recording chambers indicated on a top view of a monkey brain (gray area). *C*: the circular panels show the precise recording sites inside each recording chamber for both monkeys. The proportion of decision neurons at individual recording sites is coded on a gray scale. The locations and the density of the CMAr decision neurons are depicted on the surface to indicate their location within the recording chamber. They have also been projected to an unfolded reconstruction of the medial wall. The medial wall is reflected upward from the midline [longitudinal cerebral fissure (lcf)] so that it appears upside down. Solid lines indicate the boundaries of the lower and upper lips of the cingulate sulcus; a dashed line depicts the fundus. The arrow shows the level of the genu of the arcuate sulcus. ps, Principal sulcus; iar, inferior arcuate sulcus; sar, superior arcuate sulcus; CgG, cingulate gyrus; CgSv, ventral bank of the cingulate sulcus; CgSd, dorsal bank of the cingulate sulcus; Sgm, medial superior frontal gyrus.

For the analysis of the motor phase (see Fig. 9), the dependence of the firing rates was calculated using the factors intensity (*INT*), decision (*D*), motor action (*A*), and rule-cue (*R*) using the following equation:

$$FR = a_0 + a_{int} \times INT + a_d \times D + a_a \times A + a_r \times R$$

We also carried out a sliding SLR analysis during the time of the rule-cue appearance and the motor phase. Analysis windows of 100 ms were slid in steps of 10 ms for all of the four factors. The number of neurons and the SLR coefficients of neurons significantly encoding these factors in each analysis window were convolved with a Gaussian kernel (bin width 10 ms; step 1 ms) for the plot (see Fig. 9).

Coefficients were included in the model if the *P* value for the predictor (decision outcome or the stimulus intensity) was below the significance level of 5%. To test for the presence of multicollinearity, we determined the correlation coefficient the explanatory variables decision and intensity (*R*) and calculated the variance inflation factor (*VIF*):

$$VIF = 1/(1 - R^2)$$

$VIF > 5$ were used as cutoff values to detect too high multicollinearity (Kutner et al. 2004; O'Brien 2007). The concern of multicollinearity did not apply to any of the calculated fits. Because an additionally performed simple linear regression analysis provided comparable results, concerns that stepwise procedures might only inaccurately capture the importance of the parameters (Hendenson and Denison 1989) can be excluded.

For the comparison of the SLR coefficients among each other and between areas, the coefficients were normalized. The absolute coefficient values (a) can be written as the change of the firing rate (ΔFR) divided by the change of the factor (ΔF), which equals $\tan(\gamma)$:

$$a = \Delta FR/\Delta F = \tan(\gamma)$$

$$\gamma = \tan^{-1}(a)$$

The values are divided by the maximal possible value $\pi/2$ for γ to normalize the coefficient values between 0 and 1

$$a_{norm} = \tan^{-1}(a)/(\pi/2)$$

Classification of decision cells into "yes" and "no" neurons. Neurons showing a significant effect of decision (SLR analysis) were classified according to the modulation strength (*M*) of their firing rates during "yes" and "no" decisions. As a measure of the *M*, we used the mean absolute change of the *FR* in intervals of $t = 100$ ms, which were shifted in 10-ms steps $M = \frac{1}{n}\sum_{i=1}^{n}\left|\frac{\Delta FR_i}{\Delta t_i}\right|$. The starting point of the modulation analysis ($i = 1$) for both phases was advanced from the defined phase onset to a time point at which the firing rates for the "yes" and "no" decisions started to diverge significantly (see *Receiver operating characteristic analysis*); the analysis ended ($i = n$) at the defined offset of the respective phase. If the *M* was larger during "yes" decisions compared with the *M* during "no" decisions, the neuron was classified as a "yes" neuron. For stronger modulation during "no" decisions, the neuron was assigned to the "no" neuron class. Whether the dominant modulation of a neuron's response was an increase or a decrease of firing rate for a particular decision was determined relative to the firing rate of the other decision. For example, if a neuron increased its firing rate for a "yes" decision relative to the "no" decision and this increase was stronger than the firing rate modulation for the "no" decision, the neuron was classified as an increasing "yes" neuron.

We ensured that the number of randomly selected trials in both conditions was the same, thus excluding potential differences in firing variance caused by different numbers of trial repetitions. Moreover, the firing rate was previously convolved with a Gaussian kernel to smooth the fluctuations (bin width 150 ms, step 1 ms).

Our classification algorithm categorized most of the different neuronal response types well. Still, for a few of the neurons, the algorithm failed. The responses of all misclassified neurons had in common that the activity for the "yes" decision drastically dropped to 0 Hz and increased again after 300–400 ms during the stimulus phase, whereas the activity for the "no" response increased just slightly. These neurons clearly belong to the class of decreasing "yes" neurons, because, when the firing rate is 0 Hz for the "yes" decision, both the change of the firing rate and the *M* are 0 (because it cannot decrease more). Therefore, the slight increase during the "no" decision was considered as a stronger modulation, and these neurons were erroneously classified as "no" neurons (see Table 1; see Fig. 6, which shows

Table 1. *Classification of "yes" and "no" decision cells*

	Stimulus Phase				Delay Phase			
	"Yes" neurons		"No" neurons		"Yes" neurons		"No" neurons	
	↑	↓	↑	↓	↑	↓	↑	↓
PFC	34	23	1	0	79	25	21	3
preSMA	32	29	8	0	65	18	25	5
CMAr	4	11	1	0	13	7	7	0

Values are no. of decisions. PFC, prefrontal cortex; preSMA, presupplementary motor area; CMAr, rostral part of the cingulate motor area; ↑, increasing firing rate; ↓, decreasing firing rate.

the averaged firing rates for preSMA neurons; however, the decrease to 0 Hz is not visible in this figure because the responses are normalized). All of these misclassified neurons were excluded from further analysis.

Receiver operating characteristic analysis. Receiver operating characteristic (ROC) analysis (Green and Swets 1966) was performed over both abstract decision analysis intervals (stimulus phase and delay phase). Sliding ROC analysis was applied to consecutive overlapping time windows of 300 ms moved in 50-ms steps across the trial to characterize the temporal evolution of the abstract decision across time. We calculated the choice probability indexes (area under the ROC curve) comparing the discharge rates of salient (≥2.4% visual contrast) hit trials with discharge rates of correct rejections. Furthermore, we compared the hit trials of threshold stimuli (2.0%, 1.7%, 1.4%, 1.1% of visual contrast) with miss threshold trials. To exclude stimulus intensity biases in the analysis of threshold trials, equal numbers of trials for each stimulus intensity were included in the comparison of hit and miss trials for each cell. Choice probability values of 0.5 indicated chance-level discrimination; values > 0.5 denoted neurons with higher firing rates for hits compared with misses or correct rejections; choice probability indexes < 0.5 signified cells with higher discharge rates for misses and correct rejections. To calculate significance levels and confidence intervals, we used the bootstrapping technique. We constructed 1,000 resamples of the discharge distributions, each of which was obtained by random sampling of firing rates of both compared conditions with replacement keeping the original number of trials for each condition. We calculated the choice probability index for each resample and evaluated value of the original dataset compared with the distribution of the indexes calculated for the resamples. If 95% of the randomly generated distributions showed higher/lower choice probabilities than the original value, it was considered statistically significant ($P < 0.05$).

Response latency. We assessed the latency of the neuronal responses over an interval of 500 ms following the stimulus onset using sliding ROC analysis (50-ms windows moved by steps of 1 ms). If the choice probability index exceeded the 95% threshold of the bootstrapped data for 50 consecutive windows, the time point of the first significant window was considered the latency of the neuronal response. For the calculation of the averaged latencies, only data of neurons were included for which latency could be determined. For the SLR and ROC analyses, neurons' response latency marked the start of the stimulus analysis phase (see *Data analysis*). If no value for the response latency could be determined for a neuron, a default latency corresponding to the 75th percentile of the response latency distribution of a given recording site was used as a starting point of the stimulus phase (PFC: 179 ms; preSMA: 180 ms; CMAr: 225 ms). Equivalent results were obtained for the different classes of decision cells in the stimulus phase, if the starting point of the analysis window was set to a fixed latency of 179 ms for all PFC cells, 180 ms for all preSMA neurons, and 225 ms for all CMAr cells, resulting in cell numbers for each class of decision neurons, which were not significantly different from the numbers reported in Table 1 ($P > 0.05$, χ^2 test).

Population analysis and normalization. Spike density histograms of significantly selective neurons assigned to a particular response class were normalized and averaged. Averaged firing rates of each cell were normalized by subtracting the mean baseline activity and dividing by the standard deviation of the baseline activity. Baseline activity was derived from a 300-ms period prior to stimulus onset. For illustrative purposes, spike density histograms were convolved with a Gaussian kernel (bin width 150 ms, step size 1 ms).

RESULTS

Two monkeys were trained to perform the rule-based detection task (Fig. 1*A*). The animals were presented with a visual stimulus at nine different stimulus intensity values; in one-half of the trials, no stimulus was shown. Our experimental design assured that the monkeys could not prepare any motor response during the delay period, which followed the presentation of the visual stimulus. Only after the rule cue was presented, the monkeys could prepare a particular motor action to report the presence or absence of the stimulus. The intensities of the stimuli were chosen close to the perceptual threshold to introduce decision ambiguity. Thus the internal status of the animals determined whether the presented stimulus was detected (hit) or not (miss), or whether the absence of the stimulus was reported correctly (correct rejection) or indicated erroneously as stimulus-present trial (false alarm). Both monkeys reported in almost 100% of the trials the presence of salient stimuli. In about 90% of stimulus absent trials, the monkeys correctly rejected the presence of any stimulus; for stimuli close to the perceptual threshold animals were able to correctly detect the stimulus in a proportion of trials dependent on the intensity. The psychometric curves are depicted in Fig. 1, *B* and *C*.

Types of neurons processing the abstract decision. While the monkeys performed the task, we recorded the activity of randomly selected single neurons in the different cortical areas: we collected 520 neurons in the preSMA of the medial wall of the frontal cortex; 149 neurons were recorded from the rostral CMAr (area 24c), parts of the dorsal and ventral banks of the cingulate sulcus, anterior to the genu of the arcuate sulcus. These recordings from the preSMA and the CMAr were compared with the activity of 708 neurons recorded in the lateral PFC from both the upper and lower banks of the principal sulcus (Fig. 2, *A* and *B*) of the very same monkeys (PFC data published in Merten and Nieder 2012).

For all three areas we compared the coding of the abstract perceptual detection during the early decision phase (stimulus phase) and during the late decision processing, when any motor preparation was still excluded (delay phase, see Fig. 1*A*). We asked how the activity of the neurons was influenced by the subjective decision about the stimulus presence ("yes" decision) or absence ("no" decision) and whether and how strongly the activity was modulated by the physical properties of the presented stimulus. We applied SLR analysis to access the impact of both factors on the firing rates of hit and false alarm trials ("yes" decision) compared for all stimulus intensities to correct rejections and miss trials ("no" decision). We found that abstract decisions were processed in all three investigated brain areas. Proportions of neurons significantly encoding the monkey's judgment about the stimulus presence or absence during the stimulus and delay phases are depicted in Fig. 3

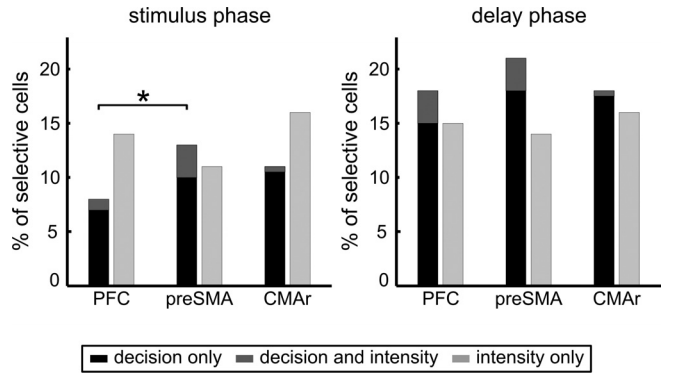

Fig. 3. Proportions of selective cells during the decision phase. The bar plots show the frequency distributions of neuron coding decision or stimulus intensity in the PFC, preSMA, and CMAr during the stimulus (*A*) and delay phase (*B*). *$P < 0.05$.

($P < 0.05$, SLR analysis). These neurons were termed "decision neurons." Significantly more cells represented the abstract decision in the preSMA compared with the PFC during the stimulus phase ($P < 0.05$, Fisher's exact test, Bonferroni corrected). In all investigated areas, the intensity of the stimulus was represented during both the stimulus and delay phase. Proportions of intensity encoding neurons are shown in Fig. 3. Few cells were modulated by both factors stimulus intensity and decision during both decision analysis phases in all areas (1–3%).

Classes of neurons encoding the abstract decision. We identified different types of decision neurons according to the active modulation of their discharge rates during "yes" and "no" decisions. This approach assured that exciting as well as suppressive effects could be detected as the dominant effect of a particular stimulus. The selectivity of a neuron was defined by the condition, which elicited the stronger modulation of the neuron's firing rate. Neurons modulating (increasing or decreasing) their activity more strongly for "yes" decisions were termed "yes" neurons; cells modulating their activity more strongly to "no" decisions were called "no" neurons (see MATERIALS AND METHODS).

During the stimulus phase, virtually all decision neurons in all three areas (PFC, preSMA, and CMAr) were classified as "yes" neurons. Figure 4*A* depicts single cells that increased their firing rates for "yes" decisions (during "hit" trials for salient stimuli), whereas the activity for "no" decisions (correct rejections in stimulus-absent trials) remained at baseline level. This activity was compared with the discharges in trials when a near-threshold stimulus was presented, and the animal decided that the stimulus was present in about one-half of the trials, but missed the stimulus in other one-half of trials. Neuronal responses for threshold trials closely resembled the responses for the decisions in salient trials and, therefore, correlated significantly with the monkey's judgment.

Some cells encoded the decision for a short period after stimulus presentation (e.g., the PFC neuron in Fig. 4*A*); other cells maintained high levels of activity for "yes" decisions throughout the delay period (e.g., the preSMA neuron in Fig. 4*A*). Neurons in Fig. 4*B* showed a transient suppression of their firing rates for "yes" decisions.

Interestingly, a population of "no" cells emerged during the delay phase (Figs. 4*D* and 5*D*) in addition to the population of "yes" cells (Figs. 4*C* and 5*C*) in all three areas. "No" neurons modulated their firing rates more strongly for "no" decisions, i.e., during correct rejections, when the stimulus was absent, and during miss trials whenever a physical stimulus remained undetected (Figs. 4*D* and 5*D*). "Yes" neurons, just as in the stimulus phase, increased (Figs. 4*C* and 5*C*) or decreased (not shown) their discharge rates more strongly for "yes" decisions in salient and threshold trials.

Our classification algorithm rarely misclassified (see MATERIALS AND METHODS) the modulation strength (M) of few cells during the stimulus phase. These cells clearly show a stronger decrease of activity for "yes" decisions compared with the modulation of activity for "no" decisions, but were erroneously classified as "no" neurons (see Table 1). The averaged responses of such cells recorded in the preSMA are displayed in Fig. 6. These cells were excluded from further analysis. Overall, decisions in the stimulus phase were processed by active "yes" neurons in the PFC, preSMA, and CMAr.

The identified decision-neuron classes and the respective numbers of cells are summarized in Table 1. Responses of decision neurons averaged for each cell class and each frontal cortex area are depicted in Fig. 5. The population analysis includes the activity of the decision neurons during false alarm trials. Mirroring activity of the hit trials, firing rates during false alarms were increased (Fig. 5*A*) or decreased (Fig. 5*B*) during the stimulus phase; in the delay phase, "yes" cells increased (Fig. 5*C*), and "no" cells remained the firing rates at baseline level (Fig. 5*D*) during erroneous "yes" decisions.

Temporal response characteristics. For all decision cells, we calculated the choice probability indexes (ROC analysis; Britten et al. 1996; Green and Swets 1966) to quantify how well the neuronal activity of decision neurons predicted the monkey's decision throughout the trial. The *bottom* panels of Fig. 4 represent the comparison of choice probabilities calculated for "yes" decisions in salient hit trials vs. "no" decisions in stimulus-absent trials (correct rejections), as well as for "yes" (hits) vs. "no" (misses) decisions in threshold trials when stimuli were presented close to the perceptual threshold. Indexes derived from threshold trials closely mirrored indexes of salient trials; values above chance level indicated the intervals during which these neurons' discharges reliably predicted the monkey's decision ($P < 0.05$, ROC analysis, bootstrapping). This effect was also present on the neuronal population level (Fig. 5).

Response latencies. We computed the latency of the neuronal responses after the onset of the stimulus. There was no difference in the response latency between neurons encoding the intensity of the stimulus (250 ms) and neurons encoding the monkey's subjective decision (231 ms) ($P > 0.05$ Mann-Whitney *U*-test). We found comparable response latencies (intensity and decision coding neurons together) in all three recorded areas: 234 ms in the PFC, 255 ms in the preSMA, and 280 ms in the CMAr ($P > 0.05$, Kruskal-Wallis test).

Strength of decision encoding. We compared the PFC, preSMA, and CMAr areas in their selectivity strength for the abstract decision encoding. Two types of measurements were used for this evaluation. First, we compared the decision SLR coefficients of decision neurons across the three areas (a_d, Fig. 7*A*). Moreover, we related the strength of the decision processing of these brain areas to their encoding strength of stimulus intensity, by intensity selective neurons (a_{int}, Fig. 7*B*). We calculated a three-way

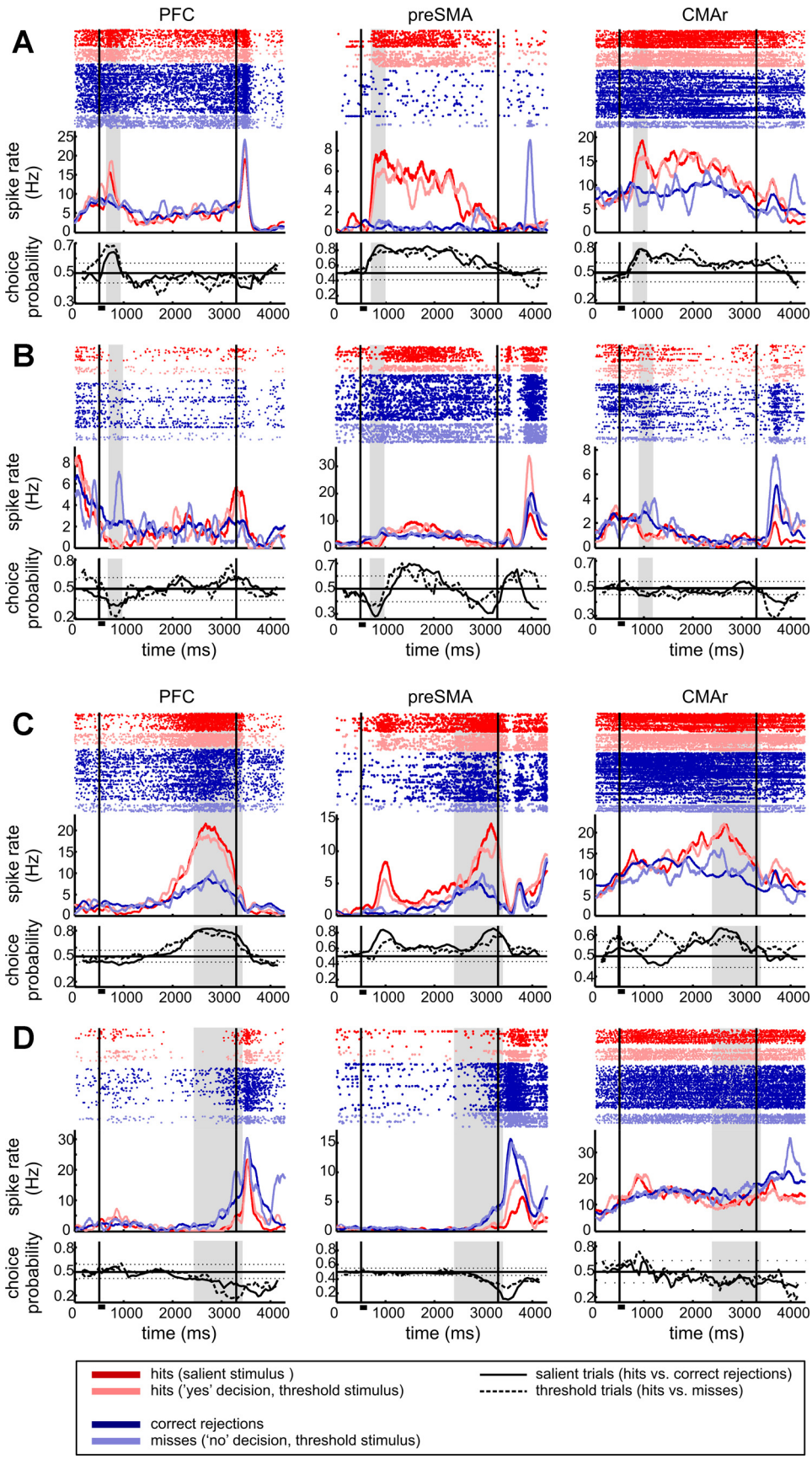

Fig. 4. Example decision neurons in the PFC, preSMA, and CMAr. Decision neurons correlated with the subjective decision of the monkey about the presence or absence of the stimulus. During the stimulus phase (analysis window highlighted by the gray shaded area), "yes" neurons encoded the decision by increasing (*A*) or decreasing (*B*) their firing rates for "stimulus present" reports of the monkey. During the delay phase, decision is encoded by active "yes" (*C*) and "no" (*D*) neurons, increasing their firing rates for "yes" (stimulus present) or "no" (stimulus absent) decisions, respectively. *Top* panels of each plot depict dot raster plots; *middle* panels represent the corresponding spike density histograms averaged and smoothed with a Gaussian kernel for illustration. The vertical black lines indicate the presentation of the stimulus (at 500 ms) and the rule cue (3,300 ms). Stimulus duration is marked by a small horizontal bar underneath the *x*-axis of each plot. *Bottom* panels show the individual neurons' choice probability indexes as a function of time. Dotted lines mark significance levels.

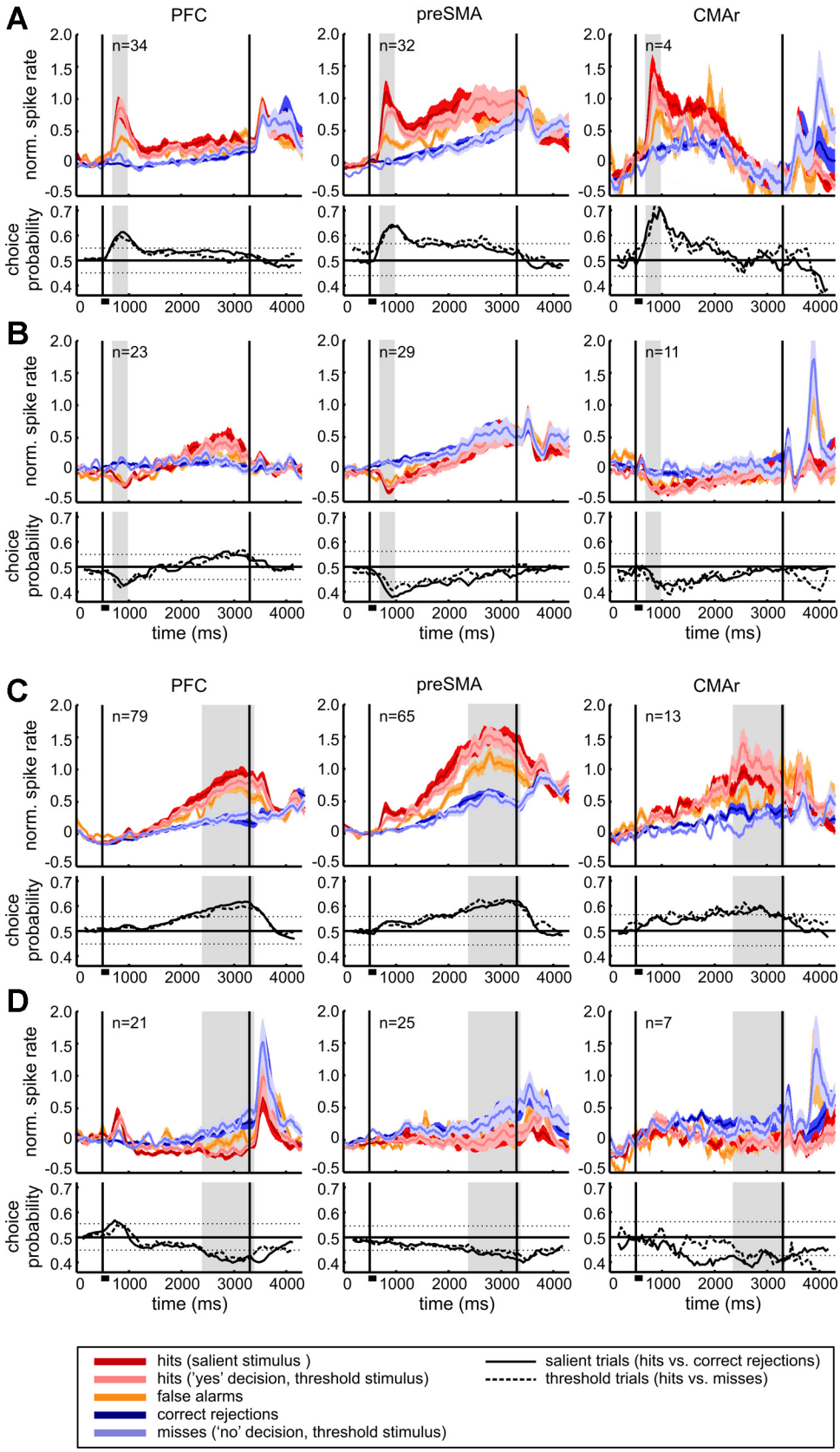

Fig. 5. Decision neurons averaged across different response classes and recording areas. *A* and *B*: normalized, averaged responses and choice probability indexes of neurons in the PFC, preSMA, and CMAr coding the "yes" decision during the sample phase. *C* and *D*: averages of neuron classes increasing their activity for "yes" decisions (*C*) or for "no" decisions (*D*) during the delay phase. Shaded regions indicate SE; *n*, number of neurons. Same layout as in Fig. 4.

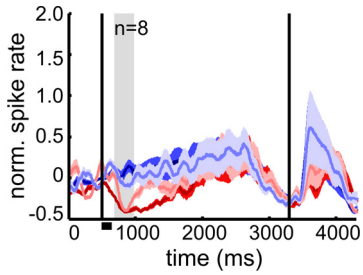

Fig. 6. Averaged responses of misclassified decision cells. Normalized and averaged responses are shown of eight preSMA neurons coding the decision during the stimulus phase, which erroneously were classified as "no" cells. The response characteristics of the average (as well as single cells, not shown) are equivalent to cells decreasing their firing rates during "yes" responses (see Fig. 5*B*; same layout as in Fig. 5).

ANOVA for the absolute values of the SLR coefficients with the following factors: neuron type (intensity or decision coding), analysis phase (stimulus or delay phase), and recording area (PFC, preSMA, CMAr). This analysis showed a significant effect of recording area (PFC: $a_d = 0.22$; preSMA $a_d = 0.27$; CMAr $a_d = 0.24$; $P < 0.05$, ANOVA). Post hoc tests revealed that preSMA showed significantly higher decision-encoding strength than PFC ($P < 0.01$, Wilcoxon test, Bonferroni corrected). No differences of decision-encoding strength were found between the analysis phases ($P > 0.05$, ANOVA). In all three areas, the encoding strength of the abstract decision ($a_d = 0.24$) was significantly larger compared with the encoding strength of stimulus intensity ($a_{int} = 0.04$; $P < 0.05$, ANOVA).

As a second measurement of the encoding strength, we used the choice probability indexes (*sc*) derived from salient and threshold trials for all recording areas during the stimulus and delay phase, respectively. For a comparison of absolute differences of choice probability indexes, a chance discrimination level 0.5 was used ($sc = |\text{choice probability} - 0.5|$). A three-way ANOVA with factors trial type (salient/threshold) × trial phase (stimulus/delay phase) × recording area (preSMA, CMAr, PFC) showed a significant effect of the recording area (see Fig. 13*C*, PFC: $sc = 0.11$; preSMA $sc = 0.14$; CMAr $sc = 0.10$; $P < 0.05$). Post hoc tests revealed that preSMA showed significantly higher decision encoding strength than PFC ($P < 0.01$, Wilcoxon test, Bonferroni corrected) and significantly higher choice probabilities than CMAr ($P < 0.05$, Wilcoxon test, Bonferroni corrected).

To access the strength of the influence of stimulus intensity on the encoding of abstract decisions, we plotted the stimulus and delay phase mean choice probability indexes of the salient hit trials and correct rejections trials against the indexes of the threshold hit trials and miss trials (Fig. 8). To visualize the influence of stimulus intensity, we plot the regression lines fitted to the indexes (goodness of fit $R^2_{adj} > 0.6$). The fitted slopes slightly deviated from 1, indicating lower choice probability values for threshold trials illustrating weak impact of stimulus intensity on decision coding. Yet this weak effect was not significant, as can be seen in the foregoing ANOVA; the factor salient/threshold choice probability was not significant ($P > 0.05$, ANOVA).

Encoding during the motor phase. To access the encoding properties of PFC, preSMA, and CMAr during the motor phase (compare Fig. 1*A*), we analyzed the selectivity of these areas for the factors decision, stimulus intensity, rule cue, and the instructed motor action using SLR analysis. The proportions of neurons selective for these factors are summarized in Table 2. Even during the motor phase after the motor action was instructed, neurons in all three areas maintain the representation of the decision. Comparable proportions of neurons encoding the decision ($P > 0.05$, Fisher's exact test) and their SLR coefficients ($P > 0.05$, Wilcoxon test) were found for all three areas. The representation of the motor action showed significant differences. The fractions of neurons encoding the motor action significantly exceeded the fraction of PFC motor coding cells in the preSMA ($P < 0.01$, Fisher's exact test, Bonferroni corrected) and the CMAr ($P < 0.05$, Fisher's exact test, Bonferroni corrected). Additionally, the SLR coefficients were significantly higher in preSMA compared with PFC neurons ($P < 0.05$, Wilcoxon test, Bonferroni corrected).

A sliding SLR analysis illustrates the time course of the encoding of the different factors (proportions of selective neurons, Fig. 9*A*; absolute SLR coefficients, Fig. 9*B*). Only 100 ms after the rule-cue onset, responsive neurons began to encode the color of the rule-cue and to a greater extent the motor response. Despite a comparably high proportion of neurons encoding the intensity of the stimulus during the motor phase (see Table 2), their SLR coefficients were negligibly small (Fig. 9*B*).

Moreover, we analyzed the neurons encoding the motor action after the rule-cue in more detail. In the PFC, significantly more motor-action neurons increased their firing rates during the hold trials, 62% (72/116), compared with the trials with bar releases, 38% (44/116) ($P < 0.05$, χ^2 test). In contrast, comparable proportions of neurons encoded hold and release motor actions in the preSMA [hold: 48% (79/163); release: 52% (84/163)] and the CMAr [hold: 55% (24/44); release: 45% (20/44)] ($P > 0.05$, χ^2 test). Proportions of neurons encoding

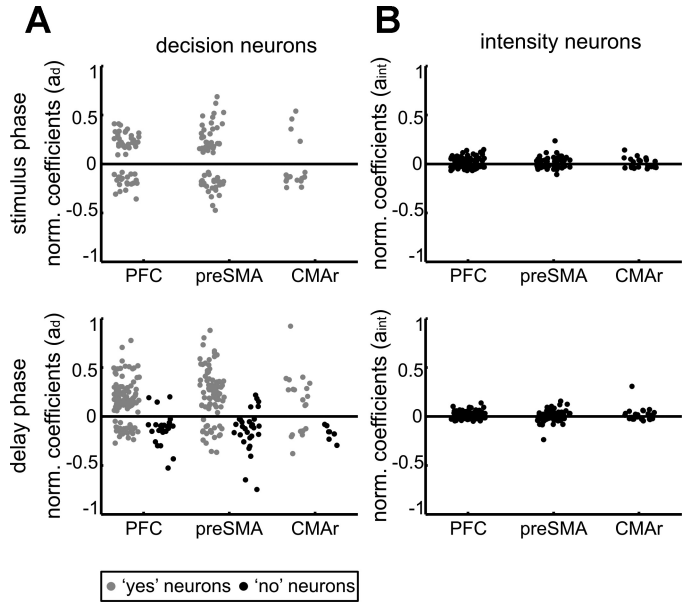

Fig. 7. Strength of decision and intensity encoding across the recorded areas. *A*: stepwise linear regression (SLR) coefficients quantify the dependence of the activity of decision neurons on monkey's subjective decision about the presence or absence of the stimulus (a_d). Decision coefficients are separated for "yes" and "no" decision neurons. *B*: this encoding strength is compared with the dependence of the firing rates of intensity neurons on stimulus intensity (a_{int}). Normalized coefficients are plotted across all recorded brain areas and both decision phases. Points are randomly shifted along the horizontal axis for clarity.

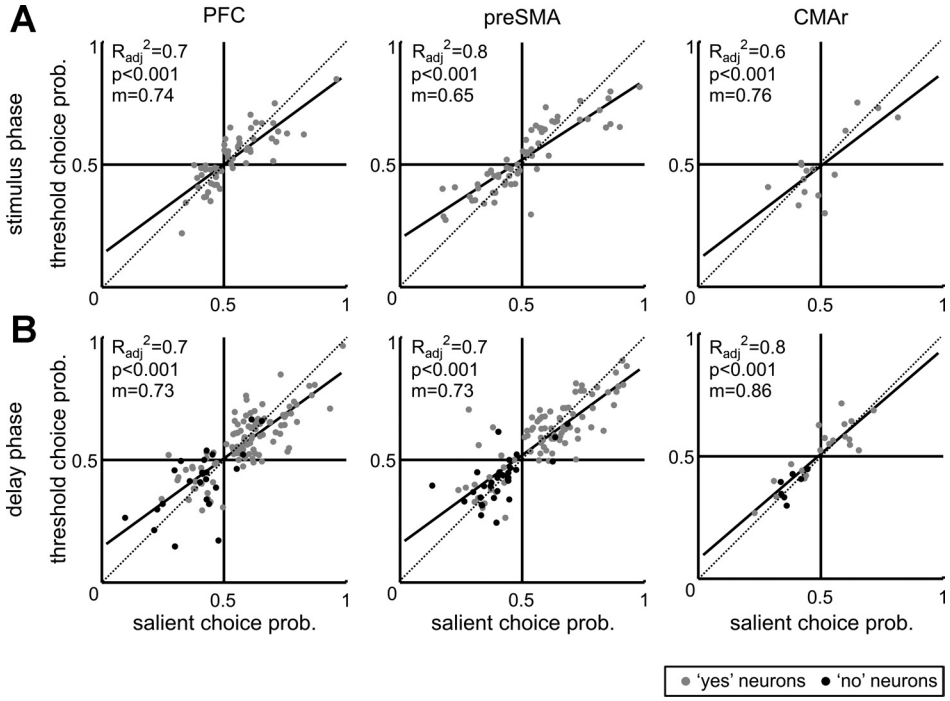

Fig. 8. Comparison of choice probability indexes for salient and threshold trials. Choice probability indexes of the salient trials are plotted against indexes of threshold trials for significant decision cells [stimulus phase (*A*); delay phase (*B*)] for all recorded brain areas. Gray points depict values of "yes" neurons; black points mark "no" neurons. Choice probability indexes > 0.5 mark cells increasing their firing rates for the type of decision they encode. Neurons decreasing the firing rate to encode the decision have choice probability indexes < 0.5. The dotted diagonal depicts the line of equality on which all points would fall, if the cells differentiated equally well between salient hits/correct rejections and threshold hits/misses. The continuous black line represents the regression line. *Insets* show goodness of fit estimation (R^2_{adj}) and the associated *P* values for H_0: $R^2_{adj} = 0$; *m*, slope of the linear fit.

both motor actions over time after the rule-cue onset are presented in Fig. 10 for all three areas.

Controls for putative motor preparation activity. Further analyses ensured that the monkeys did not adopt a strategy to solve the task based on motor preparation (see DISCUSSION). Such a strategy would involve a default preparation of a motor plan, e.g., bar release upon a "yes" decision, which is executed only if a red rule-cue is presented, but canceled if a blue rule-cue appears. Conversely, bar-holding would be prepared upon a "no" decision and changed after a blue rule-cue into a release movement. If the monkeys applied this strategy, the reaction times (RT) for red and blue rule-cues would be expected to differ drastically. For the given task design, we compared the RT for the release trials. The median RT for the "yes" decision followed by a red rule-cue (339 ms) were only 46 ms shorter compared with the RT for the "no" decision followed by a blue rule-cue (385 ms) ($P < 0.05$, Wilcoxon test). However, this difference is most likely caused by the different certainty levels of "yes" and "no" decisions. The "yes" decision (in particular for the salient trials) implies much more certainty then the "no" decision (this can be seen in the shift of the psychometric curve, Fig. 1, *B* and *C*). Accordingly, the RT for "yes" decisions followed by a red cue and a bar-release became shorter with increasing stimulus contrast and thus certainty. The RT for "yes" decisions for above-threshold stimuli (>2% visual contrast) were significantly shorter (330 ms) compared with RT of "yes" decisions for stimuli below the perceptual threshold (380 ms) ($P < 0.05$, Wilcoxon test). Thus, RTs were the same when comparing "no" decisions followed by a blue rule-cue with "yes" decisions for stimuli below perceptual threshold (around 380 ms each).

Table 2. *Proportions of neurons encoding task factors during the motor phase*

	Decision, %	Intensity, %	Action, %	Rule-cue, %
PFC	17	13	16	11
preSMA	15	16	31	15
CMAr	13	11	30	11

Moreover, if the neurons encoded a default action preparation, the firing rate should always drastically change after the rule-cue presentation if the color of a "nonprepared" movement appears and the motor plan has to be changed. An analysis of decision neurons' responses separately for each rule-cue during the motor phase argues against this possibility. As reported above (Figs. 9 and 10), the encoding of the action became the predominant response after the rule cue presentation in all three areas. However, we found decision neurons which did not encode the motor action, but continued to show the same response pattern independent on the rule-cue (Fig. 11*A*). Decision neurons that did encode the motor action during the motor phase showed both types of preferences for the motor response: "yes" and "no" decision neurons that preferred the release movement (Fig. 11*B*) and decision neurons that showed higher firing rates for the holding action (Fig. 11*C*). The presence of both types of neurons argues against the interpretation that the neurons encoded the decision in terms of a default motor preparation. This finding rather indicates that the encoding of motor action starts during the motor phase, independently of the abstract decision representation during the decision phase.

Selectivity of individual neurons during the course of the trial. Neurons in all investigated areas exhibited selectivity for all task parameters: stimulus intensity, decision, rule cue color, and action selection in the different phases during the trial. Figure 12 illustrates the selectivity of neurons for decisions during the stimulus and delay phase. Most neurons only encoded the decision during one of the analysis phases. Some neurons showed decision selectivity during both decision phases (PFC: 7%; preSMA: 15%; CMAr: 11%). Only few neurons (<1% in PFC and preSMA and none in the CMAr, data not shown) encoded three task parame-

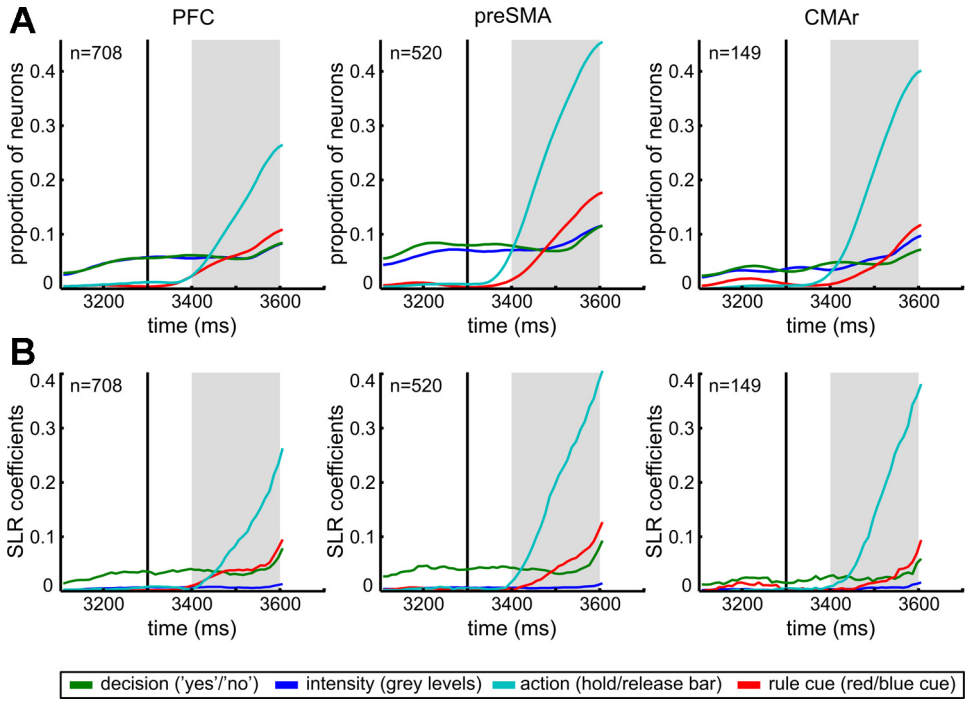

Fig. 9. Neuronal responses during the motor phase. Shown are the proportions of neurons in each recorded area significantly selective for the factors decision, stimulus intensity, motor response, and rule cue (*A*) and the absolute encoding strength of these factors across time during the motor phase (*B*). The vertical black line at 3,300 ms depicts the onset of the rule cue that instructs the action. The gray area highlights the analysis window of the motor phase, which starts 100 ms after the onset of the rule cue and lasts for 200 ms, which is the average time, after when monkeys performed an action in instructed release trials. No selectivity for the rule cue or motor action was present during the previous delay phase (until 100 ms after rule onset).

ters: decision during at least one of the decision phases and rule color and action during the motor phase. Two of these three task parameters were encoded by 13% in the PFC, 16% in the PreSMA, and 10% of the CMAr neurons.

Differences between the PFC, preSMA, and CMAr. A summary of the differences between the studied brain structures is presented in Fig. 13. A higher proportion of decision encoding neurons was identified during the early decision phase in the preSMA than in the PFC; the fraction of action encoding cells during the motor phase is higher in the preSMA and the CMAr compared with the PFC (Fig. 13*A*). The encoding strength for the motor action was also significantly larger in the preSMA than in the PFC (Fig. 13*B*). Both SLR and ROC analyses identified the preSMA as a more reliable encoder of the abstract decision compared with the PFC (Fig. 13, *B* and *C*). Additionally, the choice probabilities of the preSMA were also significantly larger compared with the CMAr (Fig. 13*C*).

Impact of spontaneous activity on decision formation. Fluctuations in spontaneous neuronal activity immediately preceding stimulus presentation might influence the firing rates of decision neurons and bias the monkeys' subjective "yes" and "no" judgments. We investigated whether the spontaneous preSMA, CMAr, and PFC activity (300-ms period prior to stimulus onset) reflected the decision during the stimulus phase. "Yes" neurons decreasing their firing rates showed significantly lower spontaneous activity preceding "yes" decisions compared with "no" decisions (preSMA: "yes" 6.4 Hz, "no" 6.7 Hz; PFC: "yes" 2.0 Hz, "no" 2.4 Hz; $P < 0.05$, paired *t*-test on ranks). However, "yes" cells increasing their discharge rates did not show such difference in spontaneous activity (preSMA: "yes" 9.3 Hz, "no" 9.2 Hz; PFC: "yes" 4.1 Hz, "no" 4.0 Hz, $P > 0.05$, paired *t*-test on ranks). No difference in spontaneous activity was found for CMAr cells (decreasing "yes" neurons: "yes" 7.1 Hz, "no" 7.2 Hz; increasing "yes" neurons: "yes" 10.6 Hz, "no" 10.3 Hz; $P > 0.05$, paired *t*-test on ranks).

DISCUSSION

In the present study, we investigated the representation of abstract detection decisions in the medial frontal areas preSMA and CMAr and compared it to the encoding of such decisions in the PFC. Both frontal areas, traditionally associated with the planning of motor activities, represented the abstract decision

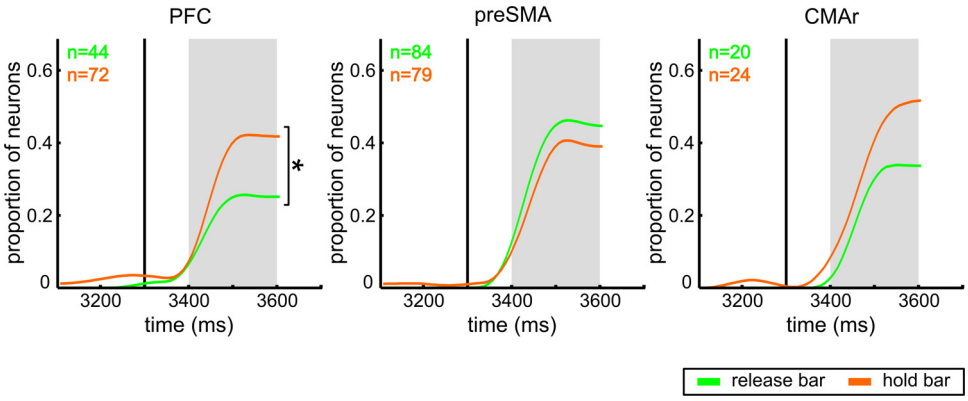

Fig. 10. Hold or release motor action encoding neurons. Temporal evolution of proportions of motor action (hold/release) encoding neurons is shown over time after the rule-cue onset (vertical black line at 3,300 ms). Significantly more neurons increased discharge during hold trials in the PFC; neuron proportions in preSMA and CMAr were not significantly different. $*P < 0.05$.

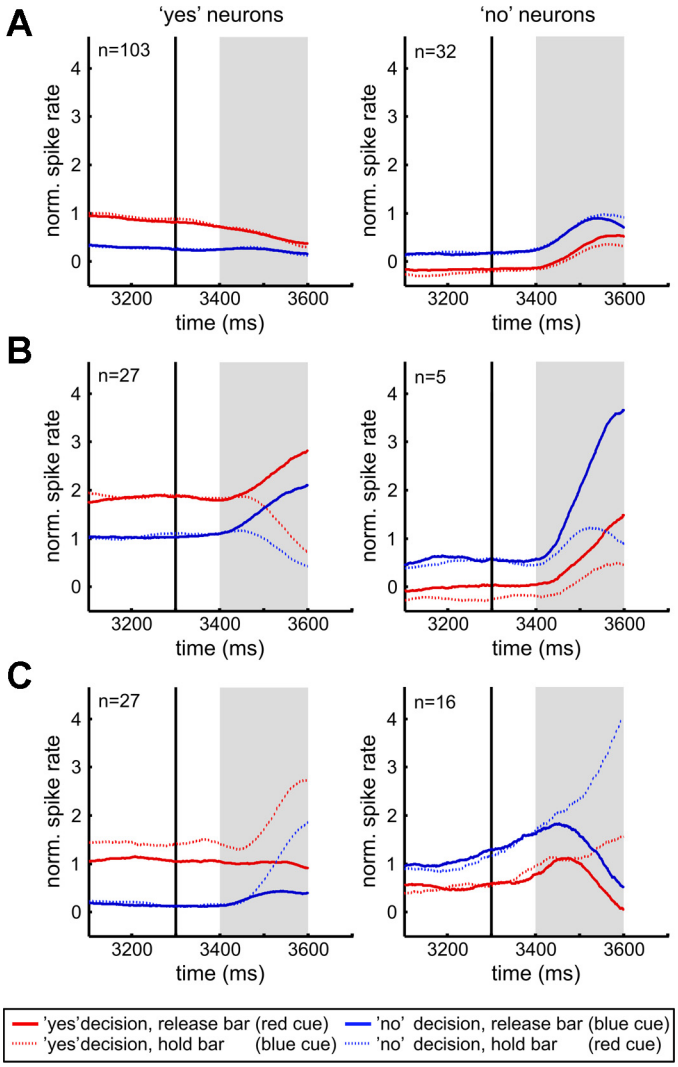

Fig. 11. Selectivity of decision neurons during cue presentation. Shown is the average neuronal activity of decision neurons in all three areas increasing their firing rates for "yes" (*left* panels) and "no" decisions (*right* panels) during the decision phase, separated according to the rue-cue (requiring a particular motor action). The vertical black line at 3,300 ms depicts the onset of the rule-cue. *A*: neurons encoding the abstract decision during the decision phase, but without selectivity for the motor action after rule-cue presentation. *B*: neurons with preference for release trials during the motor phase. *C*: neurons preferring the holding action in the motor phase.

about the stimulus presence or absence similarly to the PFC (Merten and Nieder 2012), even before any motor action instruction became available. Notably, the overall strength of abstract decision encoding was even stronger in the preSMA than in the PFC. During the motor phase, i.e., after the instruction of the motor action, preSMA and CMAr still continued to encode the decision with similar strength as the PFC, in spite of the more pronounced representation of the upcoming motor action.

Functional connectivity of the PFC, preSMA, and CMAr. The PFC has been identified as the most important cortical structure for the representation of cognitive control and highly abstract processes (Fuster 2008; Miller 2000; Miller and Cohen 2001). The PFC is thought to interpret the sensory data and recruit brain areas and circuits which generate motor commands to execute a response (Heekeren et al. 2008; Shadlen et al. 2008). The PFC involvement has been demonstrated in the processing of abstract categories (Nieder 2009, 2012; Nieder and Merten 2007; Tudusciuc and Nieder 2009; Vallentin and Nieder 2008) and rules (Bongard and Nieder 2010). Both areas, preSMA and CMAr, are reciprocally interconnected with the PFC (Bates and Goldman-Rakic 1993; Lu et al. 1994; Wang et al. 2005). This extensive cortico-cortical connectivity offers intensive communication between cognitive and motor systems. The preSMA and CMAr have been shown to play important roles in the convergence of sensory information and linking it to action (Hernández et al. 2002; Hoshi et al. 2005; Hoshi and Tanji 2006; Romo and Salinas 2003). However, the capacity of these brain structures to encode abstract processes, not linked to action, has not been investigated so far.

In more detail, the CMAr has prominent projections to the primary motor cortex (Bates and Goldman-Rakic 1993; Dum and Strick 2002; He et al. 1995) and to the corticospinal system (He et al. 1995; Hutchins et al. 1988). Stimulation studies underpin the involvement of this area in the initiation and execution of arm movements (Procyk et al. 2000; Shima et al. 1991). Furthermore, the activity of the CMAr is influenced by emotional and motivational states as it receives projections from the limbic system (Amaral and Price 1984; Morecraft and Van Hoesen 1998) and thalamic nuclei (Vogt et al. 1987; Vogt and Gabriel 1993). The anterior cingulate cortex is the main target area of the mesocortical dopamine system (Lewis 1992; Vogt and Gabriel 1993), this implicates CMAr in error detection (Gemba et al. 1986; Ito et al. 2003) and converting reward value into action (Shima and Tanji 1998).

The preSMA has sparse projections to the corticospinal system (Dum and Strick 1991; Luppino et al. 1994), no projections to the primary motor cortex, yet it has extensive connections to the nonprimary motor structures, as the CMAr (Luppino et al. 1993). This connectivity is responsible for more abstract, the so-called high-level motor functions like the sequential organization of multiple movements (Nakajima et al. 2009; Shima and Tanji 2000), updating of motor plans (Shima et al. 1996), or switching from automatic to controlled action (Isoda and Hikosaka 2007).

Our study demonstrates the involvement of both areas also in the processing of abstract decisions, which could not be represented as motor intensions. This emphasizes the important role of both premotor areas, in addition to the PFC, in cognitive control.

Processing of abstract decisions in the PFC, preSMA, and CMAr. Similar to the previously reported abstract decision processing mechanism in the PFC (Merten and Nieder 2012), we found single neurons in the preSMA and CMAr encoding the perceptual report of the animal, before the motor action was specified. The same physiological classes of decision neurons were involved: during the stimulus phase, neurons modulated their firing rates for "yes" decisions only; however, during the late delay phase, additionally, the abstract category of "no" decisions was represented actively by a group of neurons.

Applying a rule-cue, we clearly separated neuronal processing of sensory information and decision from motor preparation and action. We argue that the decision neurons we found during the stimulus and delay phase encode the decision as an abstract process. Our task design ensures that both rule-cues (red and blue) appeared equally likely for stimulus-present and stimulus-absent trials. The monkeys were trained on all four possible experimental conditions simultaneously. Therefore, it

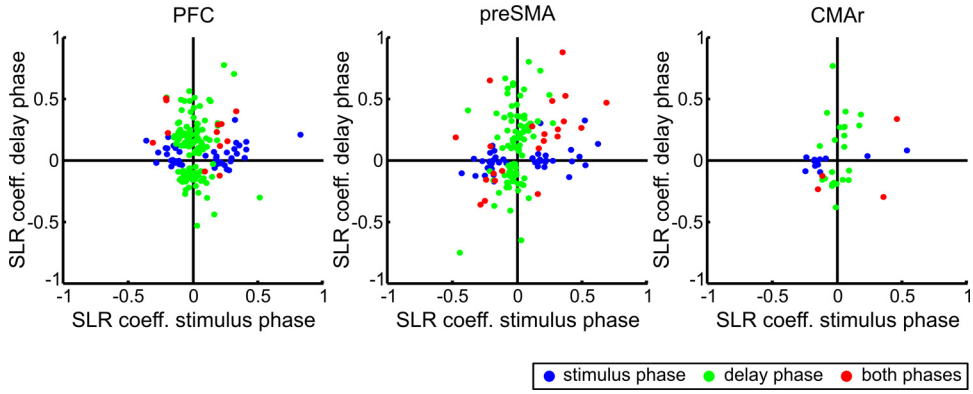

Fig. 12. Selectivity of individual neurons during both decision phases. Decision selectivity strength based on normalized SLR coefficients during the stimulus phase is plotted vs. the decision selectivity strength during the delay phase. Only few neurons (red) significantly encoded the decision during both analysis phases.

is very unlikely that the animals adapted any kind of strategy preparing for a particular movement before the rule-cue and changed this preparation after the rule-cue instruction. Neuronal activity cannot simply be related to motor preparatory activity. The decision encoding before the rule-cue must be abstract, because after the rule-cue presentation an additional evaluation of the situation and the required motor response is essential to perform the correct action.

Nevertheless, we tested the putative possibility of an alternative strategy. On average, RTs after the red rule-cue were only 46 ms shorter compared with blue rule-cue RTs. This difference is too small to be attributed to a potential change in motor planning. Countermanding reaching tasks in monkeys report durations of about 140 ms, which are required to cancel a planned hand movement (Mirabella et al. 2011; Scangos and Stuphorn 2010). The small difference in RT we found results most likely from the different certainty levels of "yes" and "no" decisions. "No" decisions have higher uncertainty levels and require longer decision times (compare behavioral performance in Fig. 1, *C* and *D*). Moreover, all possible combinations of decision neurons' selectivity for the motor action confirm that it is not simply motor preparation encoded during the decision phase, but the abstract decision. Moreover, same decision neurons are also selective for the motor action, but during the separated motor phase.

The number of neurons encoding the "yes" decision was higher than the number of neurons encoding the "no" decision during the delay phase in both monkeys. We do not believe this bias arises from the training procedure or any behavioral strategy the animals could have adapted. Both "yes" and "no" decisions have been trained simultaneously, and both decisions require the same motor actions, bar release, or hold dependent on the color cue. We rather speculate that this bias originated from the pathways and cell types involved in the decision processing. For example, there are different proportions of excitatory and inhibitory connections in the cortex, and "yes" or "no" neurons might arise from different calculations by different types of cells. This hypothesis has to be further explored using computational modeling.

In this abstract decision task, we found a different representation of detection decisions in the preSMA, CMAr, and PFC compared with action-based detection decisions (de Lafuente and Romo 2005, 2006). In the action-based framework, only one decision category, stimulus present, was encoded actively by "yes" neurons; no active encoding of stimulus-absent decisions was found. The direct comparison of the involvement of the preSMA in an abstract (our study) and action-based (de Lafuente and Romo 2005) framework demonstrates the flexibility of this area to deploy a particular processing mechanism for decisions dependent on whether an abstract decision is enforced or whether the decision can be expressed in terms of motor preparation.

Processing mechanism of abstract decisions in all the investigated frontal lobe areas (preSMA, CMAr, and PFC) by two sets of active decision neurons ("yes" and "no") is similar to the mechanism reported for the abstract discrimination decision task in the LIP (Bennur and Gold 2011). In this discrimination task, two sets of neurons encoded the decision for the rightward or the leftward motion, independent from how they encoded the motor response. Thus abstract decisions are encoded similarly to categories (Freedman and Assad 2011). Interestingly, the key task parameter "stimulus intensity," "decision," "rule cue color," and "motor action" are represented in

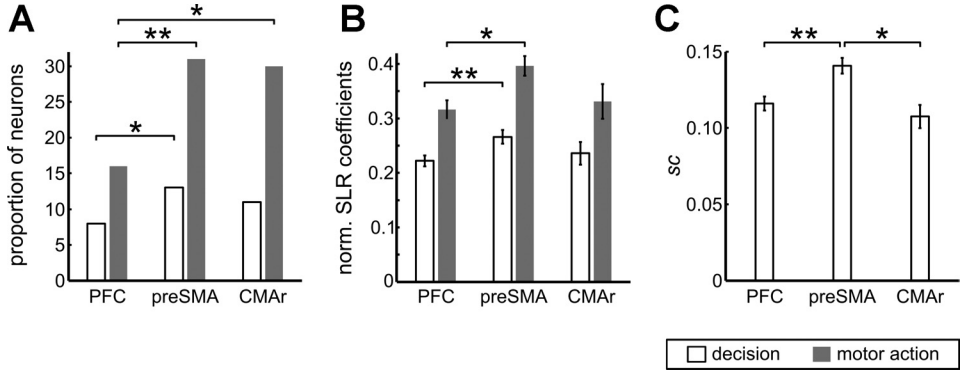

Fig. 13. Differences between PFC, preSMA, and CMAr. Comparisons are shown of quantity and quality of decision and action encoding during the decision and motor phases, respectively, for all three studied brain structures. *A*: proportions of neurons significantly encoding the decision during the early decision phase compared with the proportions of neurons encoding the motor report during the motor phase. *B*: comparison of normalized SLR coefficients for the factors decision during the decision phase and motor action during the motor phase. *C*: scaled choice probability indexes ($sc = |\text{choice probability} - 0.5|$) for decision derived for all investigated areas. Asterisks indicate significant differences (*$P < 0.05$; **$P < 0.01$, Bonferroni corrected).

both the frontal and the parietal areas. Similarly, a lower proportion of neurons in both areas represents the decision compared with neurons encoding the motor action. However, we find a predominant selectivity for just one task parameter in each individual neuron in the frontal areas. This seems to be in contrast to the involvement of LIP in abstract perceptual decisions, because LIP neurons predominantly exhibit selectivity for combinations of the task parameters (Bennur and Gold 2011). Future studies of abstract decisions in both areas simultaneously will have to compare the latencies of the abstract decision encoding and possibly the changes of representations with increasing task proficiency of the animals.

We found lower spontaneous activity of preSMA and PFC neurons that decreased their discharges for the "yes" decision, but no difference in spontaneous activity was found for "yes" cells, increasing their discharges for "yes" decisions. This result is at odds with the findings reported by deLafuente and Romo (2005), who reported increased prestimulus activity predictive for the detection success for neurons, increasing their responses for action-based decisions. The different effects of spontaneous activity on neurons increasing and decreasing their activity for the "yes" decision could possibly indicate a different origin of inputs processed by these types of neurons, and, therefore, their meaning of decision representation might require a different interpretation. Decreasing "yes" neurons possibly reflects the influence of the probabilistic fluctuations in neuronal activity prior to the stimulus presentation on the decision outcome. Another possibility might be that these neurons were influenced by the trial history. For example, a decision neuron might also be involved in reward encoding; therefore, an error in a preceding trial might decrease its prestimulus activity for the next trial.

Compared with the PFC, neurons in the preSMA exhibited stronger selectivity for abstract decisions. Similarly, a stronger selectivity of the dorsal premotor area compared with the selectivity of PFC neurons has been reported for the processing of abstract numerical rules (Vallentin et al. 2012). Overall, our finding of abstract perceptual decisions representation in the preSMA and CMAr expands the previously reported competence of these areas in intentional decisions to more abstract processes, which must be calculated independent of motor aspects and are only relevant for motor actions in later task phases.

After the presentation of the rule-cue, preSMA and CMAr continued to encode the decision to the same extent as the PFC. During the motor phase, proportionally more neurons represented the instructed motor-action in the two areas than the PFC. Moreover, the neurons in the preSMA showed stronger selectivity for motor actions than PFC neurons. Interestingly, more neurons encoded the "keep holding the bar" motor action then the "release the bar" action in the PFC, which is not the case in other investigated areas. This observation that more neurons might actively encode the maintenance of an action is consistent with the view that PFC is the source of inhibitory control in the brain (Munakata et al. 2011).

Information processing in the brain. We did not find differences in the latencies of decision encoding for PFC, preSMA, and CMAr. This result could be interpreted as abstract decision being computed in parallel in different brain areas, similar to decisions studied in action-based framework (Cisek and Kalaska 2010). Alternatively, the failure to identify differences in the latencies of the responses might constitute a resolution problem, given a limited number of neurons and notoriously difficult latency estimates in association cortexes; after all, the projections between PFC and preSMA are direct, requiring only one synapse (Wang et al. 2005).

For the accomplishment of complex operations, a serial processing mechanism of information would be advantageous. First, the brain would construct an internal representation of the stimuli, then use this information for cognitive, context-dependent computations in a nonmovement-related framework, and finally construct and execute an action plan. A processing mechanism distinct from sensory information and action appears to be implemented in all three investigated areas (preSMA, CMAr, and PFC). This seemingly serial processing is very important for cognitive functions and intelligence and is prerequisite for solving of situations, which require several steps of cognitive computation before any motor action can be carried out.

GRANTS

This study was supported by the Boehringer Ingelheim Fonds to K. Merten, the Leibniz Graduate School for Primate Neurobiology (NEUROPRIM), and a research group grant (C11/SFB 550) from the German Research Foundation to A. Nieder.

DISCLOSURES

No conflicts of interest, financial or otherwise, are declared by the author(s).

AUTHOR CONTRIBUTIONS

Author contributions: K.M. and A.N. conception and design of research; K.M. performed experiments; K.M. analyzed data; K.M. and A.N. interpreted results of experiments; K.M. prepared figures; K.M. and A.N. drafted manuscript; K.M. and A.N. edited and revised manuscript; K.M. and A.N. approved final version of manuscript.

REFERENCES

Amaral DG, Price JL. Amygdalo-cortical projections in the monkey (Macaca fascicularis). *J Comp Neurol* 230: 465–496, 1984.
Bates JF, Goldman-Rakic PS. Prefrontal connections of medial motor areas in the rhesus monkey. *J Comp Neurol* 336: 211–228, 1993.
Bennur S, Gold JI. Distinct representations of a perceptual decision and the associated oculomotor plan in the monkey lateral intraparietal area. *J Neurosci* 31: 913–921, 2011.
Bongard S, Nieder A. Basic mathematical rules are encoded by primate prefrontal cortex neurons. *Proc Natl Acad Sci USA* 107: 2277–2282, 2010.
Britten KH, Newsome WT, Shadlen MN, Celebrini S, Movshon JA. A relationship between behavioral choice and the visual responses of neurons in macaque MT. *Vis Neurosci* 13: 87–100, 1996.
Cisek P, Kalaska JF. Neural mechanisms for interacting with a world full of action choices. *Annu Rev Neurosci* 33: 269–298, 2010.
de Lafuente V, Romo R. Neuronal correlates of subjective sensory experience. *Nat Neurosci* 8: 1698–1703, 2005.
de Lafuente V, Romo R. Neural correlate of subjective sensory experience gradually builds up across cortical areas. *Proc Natl Acad Sci USA* 103: 14266–14271, 2006.
Draper NR, Smith H. *Applied Regression Analysis***. New** York: Wiley, 1966.
Dum RP, Strick PL. The origin of corticospinal projections from the premotor areas in the frontal lobe. *J Neurosci* 11: 667–689, 1991.
Dum RP, Strick PL. Motor areas in the frontal lobe of the primate. *Physiol Behav* 77: 677–682, 2002.
Freedman DJ, Assad JA. A proposed common neural mechanism for categorization and perceptual decisions. *Nat Neurosci* 14: 143–146, 2011.
Freedman DJ, Riesenhuber M, Poggio T, Miller EK. Categorical representation of visual stimuli in the primate prefrontal cortex. *Science* 291: 312–316, 2001.
Fuster JM. *The Prefrontal Cortex* (4th Ed.). London: Academic, 2008.

Gemba H, Sasaki K, Brooks VB. "Error" potentials in limbic cortex (anterior cingulate area 24) of monkeys during motor learning. *Neurosci Lett* 70: 223–227, 1986.

Gold JI, Shadlen MN. Representation of a perceptual decision in developing oculomotor commands. *Nature* 404: 390–394, 2000.

Gold JI, Shadlen MN. The influence of behavioral context on the representation of a perceptual decision in developing oculomotor commands. *J Neurosci* 23: 632–651, 2003.

Gold JI, Shadlen MN. The neural basis of decision making. *Annu Rev Neurosci* 30: 535–574, 2007.

Green DM, Swets JA. *Signal Detection Theory and Psychophysics*. New York: Wiley, 1966.

He SQ, Dum RP, Strick PL. Topographic organization of corticospinal projections from the frontal lobe: motor areas on the medial surface of the hemisphere. *J Neurosci* 15: 3284–3306, 1995.

Heekeren HR, Marrett S, Ungerleider LG. The neural systems that mediate human perceptual decision making. *Nat Rev Neurosci* 9: 467–479, 2008.

Hendenson DA, Denison DR. Stepwise regression in social and psychological research. *Psychol Rep* 64: 251–257, 1989.

Hernández A, Nácher V, Luna R, Zainos A, Lemus L, Alvarez M, Vázquez Y, Camarillo L, Romo R. Decoding a perceptual decision process across cortex. *Neuron* 66: 300–314, 2010.

Hernández A, Zainos A, Romo R. Temporal evolution of a decision-making process in medial premotor cortex. *Neuron* 33: 959–972, 2002.

Horwitz GD, Newsome WT. Separate signals for target selection and movement specification in the superior colliculus. *Science* 284: 1158–1161, 1999.

Hoshi E, Sawamura H, Tanji J. Neurons in the rostral cingulate motor area monitor multiple phases of visuomotor behavior with modest parametric selectivity. *J Neurophysiol* 94: 640–656, 2005.

Hoshi E, Tanji J. Differential involvement of neurons in the dorsal and ventral premotor cortex during processing of visual signals for action planning. *J Neurophysiol* 95: 3596–3616, 2006.

Hutchins KD, Martino AM, Strick PL. Corticospinal projections from the medial wall of the hemisphere. *Exp Brain Res* 71: 667–672, 1988.

Isoda M, Hikosaka O. Switching from automatic to controlled action by monkey medial frontal cortex. *Nat Neurosci* 10: 240–248, 2007.

Ito S, Stuphorn V, Brown JW, Schall JD. Performance monitoring by the anterior cingulate cortex during saccade countermanding. *Science* 302: 120–122, 2003.

Kim JN, Shadlen MN. Neural correlates of a decision in the dorsolateral prefrontal cortex of the macaque. *Nat Neurosci* 2: 176–185, 1999.

Kutner MH, Nachtsheim C, Neter J. *Applied Linear Regression Models*. Irwin, CA: McGraw-Hill, 2004.

Lemus L, Hernández A, Romo R. Neural encoding of auditory discrimination in ventral premotor cortex. *Proc Natl Acad Sci USA* 106: 14640–14645, 2009.

Lewis DA. The catecholaminergic innervation of primate prefrontal cortex. *J Neural Transm Suppl* 36: 179–200, 1992.

Lu MT, Preston JB, Strick PL. Interconnections between the prefrontal cortex and the premotor areas in the frontal lobe. *J Comp Neurol* 341: 375–392, 1994.

Luppino G, Matelli M, Camarda R, Rizzolatti G. Corticocortical connections of area F3 (SMA-proper) and area F6 (pre-SMA) in the macaque monkey. *J Comp Neurol* 338: 114–140, 1993.

Luppino G, Matelli M, Camarda R, Rizzolatti G. Corticospinal projections from mesial frontal and cingulate areas in the monkey. *Neuroreport* 5: 2545–2548, 1994.

Merten K, Nieder A. Active encoding of decisions about stimulus absence in primate prefrontal cortex neurons. *Proc Natl Acad Sci USA* 109: 6289–6294, 2012.

Miller EK, Cohen JD. An integrative theory of prefrontal cortex function. *Annu Rev Neurosci* 24: 167–202, 2001.

Miller EK. The prefrontal cortex and cognitive control. *Nat Rev Neurosci* 1: 59–65, 2000.

Mirabella G, Pani P, Ferraina S. Neural correlates of cognitive control of reaching movements in the dorsal premotor cortex of rhesus monkeys. *J Neurophysiol* 106: 1454–1466, 2011.

Morecraft RJ, Van Hoesen GW. Convergence of limbic input to the cingulate motor cortex in the rhesus monkey. *Brain Res Bull* 45: 209–232, 1998.

Mountcastle VB, Talbot WH, Sakata H, Hyvärinen J. Cortical neuronal mechanisms in flutter-vibration studied in unanesthetized monkeys. Neuronal periodicity and frequency discrimination. *J Neurophysiol* 32: 452–484, 1969.

Munakata Y, Herd SA, Chatham CH, Depue BE, Banich MT, O'Reilly RC. A unified framework for inhibitory control. *Trends Cogn Sci* 15: 453–459, 2011.

Nakajima T, Hosaka R, Mushiake H, Tanji J. Covert representation of second-next movement in the pre-supplementary motor area of monkeys. *J Neurophysiol* 101: 1883–1889, 2009.

Nieder A, Merten K. A labeled-line code for small and large numerosities in the monkey prefrontal cortex. *J Neurosci* 27: 5986–5993, 2007.

Nieder A. Prefrontal cortex and the evolution of symbolic reference. *Curr Opin Neurobiol* 19: 99–108, 2009.

Nieder A. Supramodal numerosity selectivity of neurons in primate prefrontal and posterior parietal cortices. *Proc Natl Acad Sci USA* 109: 11860–11865, 2012.

Nieder A. Coding of abstract quantity by "number neurons" of the primate brain. *J Comp Physiol A* 199: 1–16, 2013.

O'Brien RM. A caution regarding rules of thumb for variance inflation factors. *Qual Quant* 41: 673–690, 2007.

Pardo-Vazquez JL, Leboran V, Acuña C. Neural correlates of decisions and their outcomes in the ventral premotor cortex. *J Neurosci* 28: 12396–12408, 2008.

Picard N, Strick PL. Motor areas of the medial wall: a review of their location and functional activation. *Cereb Cortex* 6: 342–353, 1996.

Procyk E, Tanaka YL, Joseph JP. Anterior cingulate activity during routine and non-routine sequential behaviors in macaques. *Nat Neurosci* 3: 502–508, 2000.

Roitman JD, Shadlen MN. Response of neurons in the lateral intraparietal area during a combined visual discrimination reaction time task. *J Neurosci* 22: 9475–9489, 2002.

Romo R, Hernández A, Zainos A. Neuronal correlates of a perceptual decision in ventral premotor cortex. *Neuron* 41: 165–173, 2004.

Romo R, Salinas E. Flutter discrimination: neural codes, perception, memory and decision making. *Nat Rev Neurosci* 4: 203–218, 2003.

Scangos KW, Stuphorn V. Medial frontal cortex motivates but does not control movement initiation in the countermanding task. *J Neurosci* 30: 1968–1982, 2010.

Shadlen M, Kiani R, Hanks T, Churchland A. Neurobiology of decision making: An intentional framework. In: *Better Than Conscious? Decision Making, the Human Mind, and Implications For Institutions*, edited by Engel C, Wolf S. Cambridge, MA: MIT Press, 2008.

Shadlen MN, Newsome WT. Neural basis of a perceptual decision in the parietal cortex (area LIP) of the rhesus monkey. *J Neurophysiol* 86: 1916–1936, 2001.

Shima K, Aya K, Mushiake H, Inase M, Aizawa H, Tanji J. Two movement-related foci in the primate cingulate cortex observed in signal-triggered and self-paced forelimb movements. *J Neurophysiol* 65: 188–202, 1991.

Shima K, Mushiake H, Saito N, Tanji J. Role for cells in the presupplementary motor area in updating motor plans. *Proc Natl Acad Sci USA* 93: 8694–8698, 1996.

Shima K, Tanji J. Role for cingulate motor area cells in voluntary movement selection based on reward. *Science* 282: 1335–1338, 1998.

Shima K, Tanji J. Neuronal activity in the supplementary and presupplementary motor areas for temporal organization of multiple movements. *J Neurophysiol* 84: 2148–2160, 2000.

Tanji J. The supplementary motor area in the cerebral cortex. *Neurosci Res* 19: 251–268, 1994.

Tudusciuc O, Nieder A. Contributions of primate prefrontal and posterior parietal cortices to length and numerosity representation. *J Neurophysiol* 101: 2984–2994, 2009.

Vallentin D, Bongard S, Nieder A. Numerical rule coding in the prefrontal, premotor and posterior parietal cortices of macaques. *J Neurosci* 32: 6621–6630, 2012.

Vallentin D, Nieder A. Behavioral and prefrontal representation of spatial proportions in the monkey. *Curr Biol* 18: 1420–1425, 2008.

Vogt BA, Gabriel M. *Neurobiology of Cingulate Cortex and Limbic Thalamus*. Boston, MA: Birkhauser, 1993.

Vogt BA, Pandya DN, Rosene DL. Cingulate cortex of the rhesus monkey. I. Cytoarchitecture and thalamic afferents. *J Comp Neurol* 262: 256–270, 1987.

Wallis JD, Anderson KC, Miller EK. Single neurons in prefrontal cortex encode abstract rules. *Nature* 411: 953–956, 2001.

Wang Y, Isoda M, Matsuzaka Y, Shima K, Tanji J. Prefrontal cortical cells projecting to the supplementary eye field and presupplementary motor area in the monkey. *Neurosci Res* 53: 1–7, 2005.